

Thermosolutal Convection in High-Aspect-Ratio Enclosures

(NASA-TM-100803) THERMOSOLUTAL CONVECTION
IN HIGH-ASPECT-RATIO ENCLOSURES (NASA)
14 p

CSCL 20D

N88-18871

Unclass
G3/34 0128898

L.W. Wang
Lewis Research Center
Cleveland, Ohio

and

C.T. Chen
National Cheng Kung University
Taiwan, Republic of China

Prepared for the
25th National Heat Transfer Conference
sponsored by the American Society of Mechanical Engineers
Houston, Texas, July 24-27, 1988.



THERMOSOLUTAL CONVECTION IN HIGH-ASPECT-RATIO ENCLOSURES

L.W. Wang*

National Aeronautics and Space Administration
Lewis Research Center
Cleveland, Ohio 44135

and

C.T. Chen

Institute of Aeronautics and Astronautics
National Cheng Kung University
Taiwan, Republic of China

SUMMARY

Convection in high-aspect-ratio rectangular enclosures with combined horizontal temperature and concentration gradients is studied experimentally. An electrochemical system is employed to impose the concentration gradients. The solutal buoyancy force either opposes or augments the thermal buoyancy force. Due to a large difference between the thermal and solutal diffusion rates the flow possesses double-diffusive characteristics. Various complex flow patterns are observed with different experimental conditions.

INTRODUCTION

The purpose of the present study is to investigate flows resulting from buoyancy forces due a combination of temperature and species concentration effects in enclosures.

Convection in enclosures has many applications in diverse fields; for example, thermal insulation engineering, geophysics, and astrophysics. The geophysicist's interest lies in the fact that in natural geothermal phenomena temperature and concentration gradients induce density changes in the fluid which in turn lead to buoyancy-driven fluid motion. The buoyancy effect is known to play an important part in fluid motion through geothermal systems.

Convection in which the buoyant forces are due both to temperature and concentration gradients is generally referred to as thermosolutal convection or double-diffusive convection. As pointed out by Ostrach (1980), various modes of convection are possible depending on how temperature and concentration gradients are oriented relative to each other as well as to gravity. Much attention has been given to the situation in which stratified fluids are subjected to imposed vertical temperature gradients in order to explain some unusual oceanographic phenomena (e.g., Turner, 1974, Wang et al., 1987). For the same reason convection in stratified fluids with imposed horizontal temperature gradients has also been investigated (Ostrach, 1980).

Thermosolutal convection is also important in crystal growth processes (Ostrach, 1983). The transport process in the fluid phase during the growth of

*National Research Council - NASA Research Associate, on leave from the Institute of Aeronautics and Astronautics, National Cheng Kung University, Taiwan, Republic of China.

a crystal has a profound influence on the structure and quality of the solid phase. With the need for ever more perfect crystals, attention has begun to be focused on the role of convection in crystal growth. In many crystal growth techniques there are both temperature and concentration gradients in the fluid that can lead to buoyancy-driven convection. In some horizontal growth techniques (e.g., horizontal Bridgman) the fluid phase is subjected to horizontal temperature and concentration gradients. Several investigators in the past studied thermosolutal convection in an enclosure with combined horizontal temperature and concentration gradients in low-aspect-ratio enclosures (Wang et al., 1982, 1985, 1986). Extensive experimental and theoretical work is still needed to understand convection in an enclosure with combined driving forces. The present work is to study convection with temperature and concentration gradient normal to the gravity vector in electrochemical systems in high-aspect-ratio enclosures. Its main objective is to obtain more information on the resultant flows under various parametric conditions.

An electrochemical method based on a diffusion-controlled electrode reaction is employed in the present work for creating the concentration gradients. The horizontal temperature and concentration gradients are imposed in such a way that their effects on the flow are either opposing or augmenting. The resulting flow structures are studied under various conditions.

Since the main object of the present study is to obtain more information on convection due to the combined effects of temperature and concentration gradients in enclosures, the parametric ranges studied herein are mainly dictated by the electrochemical system employed to impose concentration gradients.

EXPERIMENTAL DESIGN

Dimensionless Parameters

Based on the basic differential equations for convection in an enclosure with thermal and solutal buoyancy forces (fig. 1) it can be shown that the following dimensionless parameters are important in the problem.

$$Gr_T = \frac{g\beta \Delta TH^3}{v^2} \text{ thermal Grashof number}$$

$$Pr = \frac{v}{\alpha} \quad \text{Prandtl number}$$

$$Sc = \frac{v}{D} \quad \text{Schmidt number}$$

$$N = \frac{\beta}{\beta} \frac{\Delta C}{\Delta T} \quad \text{buoyancy ratio}$$

$$Ar = \frac{H}{L} \quad \text{aspect ratio}$$

where g is the gravitational acceleration, v is the fluid kinematic viscosity, α the thermal diffusivity, and D the diffusion coefficient. The height and width of the enclosure are H and L , respectively. ΔT and ΔC are the

imposed temperature and concentration differences, respectively, between the two horizontal walls separated by H . Density variation due to temperature is represented by the volumetric thermal expansion coefficient β , and that due to concentration by the volumetric solutal expansion coefficient $\bar{\beta}$. Instead of the (Gr_T, N) combination the (Gr_T, Gr_S) combination is sometimes used, where Gr_S is defined as $Gr_S = g\bar{\beta} \Delta CH^3/v^2 = N Gr_T$, solutal Grashof number.

Test Apparatus

A sketch of the present experimental system is given in figure 1. The test cell is a rectangular enclosure. The two vertical plates are made of 0.7 cm thick copper plates and used as electrodes. An electrical heating mat is bonded to the back of one of the copper plates, and the other plate is cooled by circulating water from a constant-temperature bath. The other walls of the cell are made of 0.64 cm-thick plexiglas. The whole setup is enclosed by fiberglass insulation to minimize the heat loss from the system to the surroundings. Some parts of the insulation can be removed to facilitate qualitative-flow structure observation. Three thermocouples are imbedded in each of the copper walls to determine the wall temperature. The width (L) of the test cell is 7.6 cm and the height is variable so that a range of aspect ratio can be covered.

A copper sulphate solution is used as electrolyte. When a voltage is applied to the electrodes, copper dissolves into the solution at the anode and is deposited at the cathode. As a result the density of the fluid near the cathode (anode) becomes lower (higher) than that of the bulk of the solution. The migration of the cupric ions in the electrical field is eliminated by adding sulphuric acid to the solution, which acts as a supporting electrolyte, and thus the transport of the cupric ions in the cell is controlled only by diffusion and convection. In the experiment the concentration of $CuSO_4$ varies from 0.05 to 0.08 M. The acidity of the solution is kept constant at 1.5 M H_2SO_4 . The physical properties of the solution are taken from Wilke et al. (1953). The thermal properties of this dilute solution are close to water.

The auxillary system consists of a dc power supply, instruments to measure the total current and potential in the cell, and a variable resistance to control the current.

Test Procedure

Although the temperatures of the copper walls can be easily measured by thermocouples, the concentration levels at the walls cannot be so easily determined. One relatively simple way to specify the concentration level at the cathode wall in the present system is to adjust the cell potential in such a way that the saturation current (limiting current) is obtained. Under the limiting-current condition the ion concentration at the cathode surface is zero, in other words the change in concentration across the solutal boundary layer along the cathode ((ΔC) cathode) is C_b , where C_b is the concentration level in the bulk fluid. Since the net mass fluxes at the cathode and anode are considered to be equal and since the concentration outside the solutal boundary layers of both walls is C_b , it is reasonable to expect that the average change in concentration across the solutal boundary layer along the anode

(ΔC) anode) is nearly equal to (ΔC) cathode. Then the overall concentration difference across the cell is $\Delta C = (\Delta C)$ cathode + (ΔC) anode = $2C_b$, and thus Grs is defined based on $\Delta C = 2C_b$ in the present work. The above concept assumes that C_b remains constant, but as convection develops in the cell, the concentration level becomes nonuniform in the bulk region, and only on the average the bulk concentration level remains constant. Moreover, due to electrolysis the copper wall surfaces become rough slowly with time, which means the current densities at the walls decrease and the condition at the cathode deviates gradually from the limiting-current condition. For this reason the duration of each run is limited to maximum 4 to 5 hr, far shorter than the time required to attain steady solutal convection (≈ 500 hr). In the present cases, the electrochemical system is started after the thermal convection becomes steady. If the system is started in other ways (e.g., the electrochemical system is started first and then a temperature gradient is imposed), the concentration boundary conditions become less well-defined, since the limiting current has been found to change significantly with time as thermal convection develops in the cell. The flow patterns are studies by flow visualization. To visualize local flow structures, laser light is employed. The optical technique is shadowgraphs.

RESULTS AND DISCUSSION

Since this is a basically time-dependent problem, it may be expected to illustrate the flow structures by showing a series of shadowgraphs in time-sequence. However, the transport processes are relatively slow for the present system and the flow structure does not change significantly after the electrochemical system is started for 0.5 to 5 hr during each run. Therefore a number of photographs taken of sections of cell within a 3 min interval can be assembled together to adequately indicate the observed flow field (figs. 2 and 3). The shadowgraphs showing the entire flow at one instant is desired but technically more difficult and not necessary for the present work.

In the cooperating cases it could be anticipated that the flow structures are somewhat similar to those in purely thermal or solutal cases, i.e., unicellular flows. However, they are found to be more complex. Under certain conditions a layered flow pattern appears. The sketches of typical layered flow patterns observed by shadowgraphs for cooperating cases are given in figures 2 and 3. We think the flow along the cold anode is down to the bottom of the tank initially. But because of the box-filling process, a stably stratified fluid layer is built in the test section. Then the multilayered convection cells started because of the effect of sideways heating of a density gradient. Also we have found that secondary cells appear near each vertical wall by using optical visualization techniques. In the cells near the cold anode the secondary cell flows are counterclockwise (figs. 2 and 3). It is not easy to understand how the conditions for the cooperating cases are conducive to the formation of fingers, as implied by figure 6. The fluid turning the corner at the bottom of the anode seems copper rich and hence should resist acquisition of the positive buoyancy required for development of the secondary cells. The reason for the cells formation is speculated to be as follows. Consider the region near the cold anode. Due to thermal convection less-concentrated fluid at the top of the test section in the thermal boundary layer is brought down along the anode in each layer. But after the fluid near the anode turns around the bottom of each layer and moves out of the thermal boundary layer, the temperature increases while the concentration level is nearly constant, due to the

fact that the thermal diffusion process is much faster than the solutal diffusion process in the present experiment. As a result, the flow acquires upward buoyancy after the turning and secondary cells form. It is noted that the cells do not exist in the initial thermal convection and appear only after the addition of solutal convection.

It is interesting that flow structures similar to those described above are observed even when the two body forces opposed. The layered flow appears also in the opposing cases, see figures 4 and 5. We also found that secondary cells exist for opposing cases. Due to shear exerted by the flow in the thermal boundary layer along, for example, the hot anode, the fluid in the solutal boundary layer is carried upward against the buoyancy force which acts downward in the solutal boundary layer. However, when the flow near the hot anode turns around the top of each layer, the thermal convection slows down and the shear force associated with it decreases. Consequently, some of the heavy fluid goes down, resulting in secondary chaotic turbulent cells near the anode (figs. 4 and 5). Therefore, the flow structures in figures 4 and 5 for the opposing cases are similar to that in figures 2 and 3 for the cooperating cases, but the reasons for the appearance of the secondary cells are different in both cases. Secondary cells for cases can be seen in the layered flow structure. Due to the aforementioned complex flow structure in these cases, one might expect some kind of flow instability under certain conditions. That turns out to be the case. Shown in figures 6 to 8 are some instability (fingering flow) cases. Fingering convection usually refers to long, cellular convection due to warm, salty fluid above cold, fresh fluid. What we see in the shadowgraphs in the present work could be manifestations of such instabilities. For fixed solutal Grashof number and aspect ratio when the buoyancy ratio is reduced (thermal Grashof number increased), the fingers near the anode appear at the lower position for cooperating cases (figs. 6 and 7) and at a higher position for opposing cases (fig. 8).

In figures 9 and 10, the temperature distributions measured at the mid-section are presented. As the layers develop, the initial profile due to pure thermal convection becomes quite distorted. This offers at least indirect evidence of layered flow structures. The experimental error in the value of $T^* (= (T - T_b) / (T_u - T_b))$ was estimated to be ± 4 percent, where T_b , T_u are the bottom and upper wall temperatures at purely thermal steady state conditions.

CONCLUSION

The purpose of the present experimental study is to investigate the effects of imposing horizontal concentration gradients on steady thermal convection in high-aspect-ratio enclosures. The temperature and concentration gradients are imposed in such a way that their effects on the flow are either opposing or cooperating. The ranges of the parameters studied herein are $Sc = 2100$, $Pr = 7.0$, $Gr_S = 1.52 \times 10^7 - 1.28 \times 10^9$, $Gr_T = 5.01 \times 10^7 - 5.01 \times 10^8$, and $Ar = 3, 7$. Due to double-diffusive phenomena, various flow patterns appear in the enclosures. It is found that both cases the interaction between the temperature and concentration field may cause secondary cells near two end walls. Secondary cells for opposing cases can be seen in the layered flow structure. One important discovery in the present work is that some instability (fingering convection) may appear near the copper plate. Also the positions that fingers appear along the copper plate are dependent on N for fixed Ar and Gr_S .

Most of this work is qualitative but it represents a first step in gaining an understanding of confined flows due to both temperature and concentration gradients in high-aspect-ratio enclosures.

ACKNOWLEDGMENT

The preparation of this paper was made possible by the National Research Council Program. NASA Lewis Research Center has provided support for L.W. Wang's research on the related topics. The authors are thankful to the chief of Microgravity Science and Technology Branch, Mr. J.A. Salzman, for the opportunity.

The authors wish to acknowledge the help of Dr. An-Ti Chai of NASA Lewis Research Center. The communications with him in this topic have been both stimulating and encouraging.

REFERENCES

1. Kamotani, Y., Wang, L.W., Ostrach, S., and Jiang, H.D., 1985, "Experimental Study of Natural Convection in Shallow Enclosures With Horizontal Temperature and Concentration Gradients," International Journal of Heat and Mass Transfer, Vol. 28, pp. 165-173.
2. Ostrach, S., 1980, "Natural Convection With Combined Driving Forces," PCH: Physico Chemical Hydrodynamics, Vol. 1, pp. 233-247.
3. Ostrach, S., 1983, "Fluid Mechanics in Crystal Growth -- the 1982 Freeman Scholar Lecture," Journal of Fluids Engineering, Vol. 105, pp. 5-20.
4. Turner, J.S., 1974, "Double-Diffusive Phenomena," Annual Review of Fluid Mechanics, M. VanDyke, W.G. Vincenti, and J.V. Wehausen, eds., Annual Reviews Inc., Palo Alto, CA, Vol. 6, pp. 37-56.
5. Wang, L.W., Kamotani, Y., and Ostrach, S., 1982, "Experimental Study of Natural Convection in a Shallow Horizontal Cavity With Different End Temperatures and Concentrations," Report FTAS/TR-82-164, Case Western Reserve University.
6. Wang, L.W. and Chuang, P.C., 1986, "Flow Patterns of Natural Convection in Enclosures With Horizontal Temperature and Concentration Gradients," Heat Transfer 1986, C.L. Tien, V.P. Carey, and J.K. Ferrell, eds., Hemisphere Publishing Corp., Washington, D.C., Vol. 4, pp. 1477-1482.
7. Wang, L.W., Chen, C.T., and Chen, J.J., 1987, "Flow Patterns of Convection in Enclosures With Vertical Temperature and Concentration Gradients," Presented at the Joint ASME/JSME Thermal Engineering Conference, Mar.
8. Wilke, C.R., Eisenberg, M., and Tobias, C.W. 1953, "Correlation of Limiting Currents Under Free Convection Conditions," Journal of the Electrochemical Society, Vol. 100, pp. 513-523.

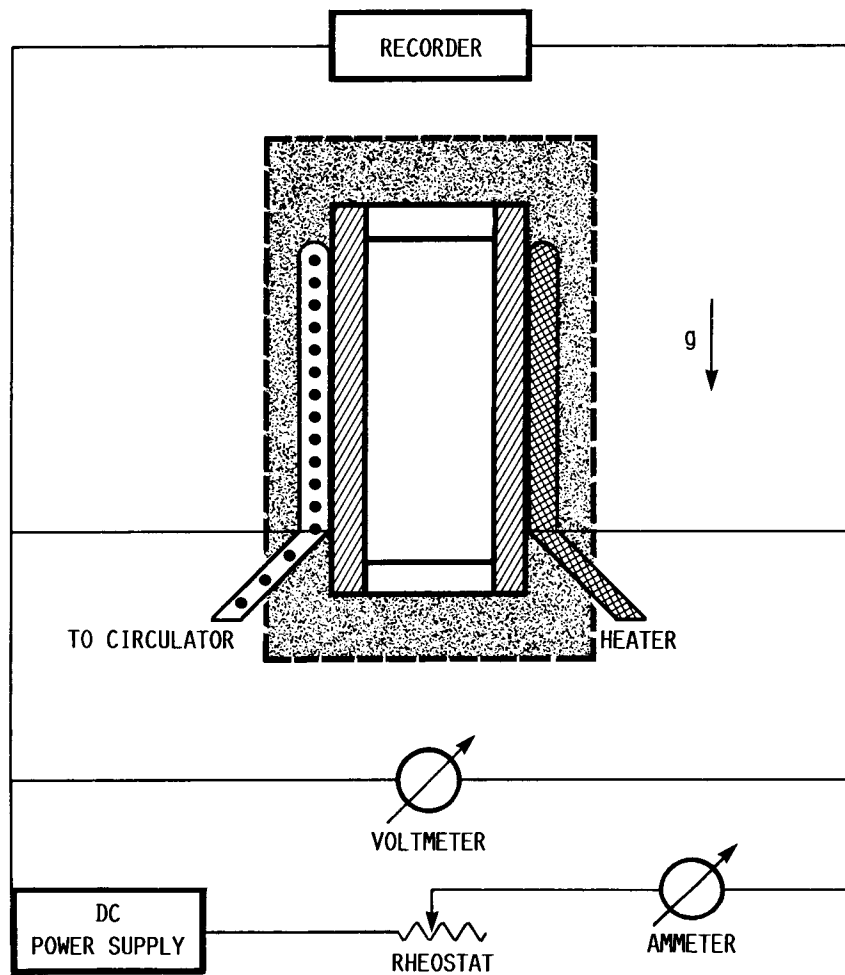


FIGURE 1. - ILLUSTRATION OF TEST CELL AND ELECTRIC CIRCUIT.

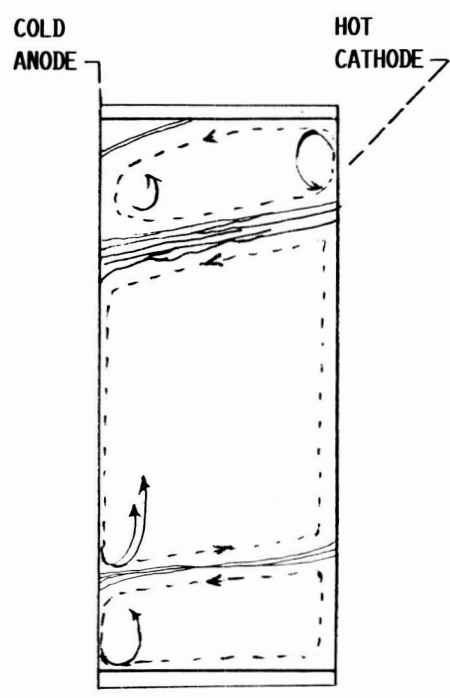
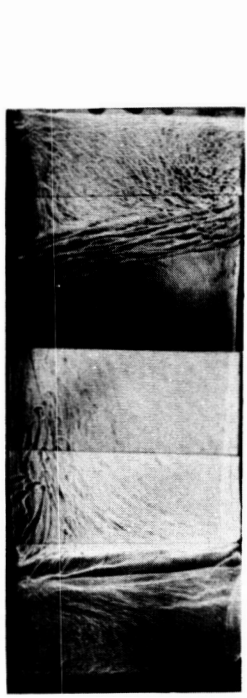


FIGURE 2. - FLOW STRUCTURE FOR COOPERATING CASE WITH
 $Ar = 3$, $Gr_T = 1.94 \times 10^8$, $Gr_S = 3.89 \times 10^8$.

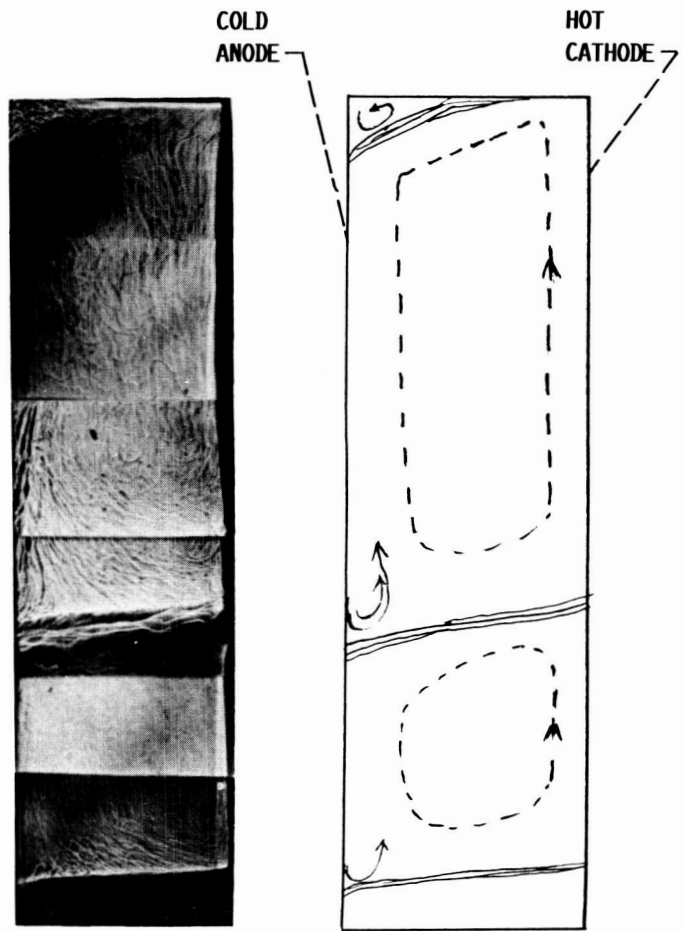


FIGURE 3. - FLOW STRUCTURE FOR COOPERATING CASE WITH
 $Ar = 7$, $Gr_T = 1.34 \times 10^8$, $Gr_S = 1.28 \times 10^9$.

ORIGINAL PAGE IS
OF POOR QUALITY

ORIGINAL PAGE IS
OF POOR QUALITY

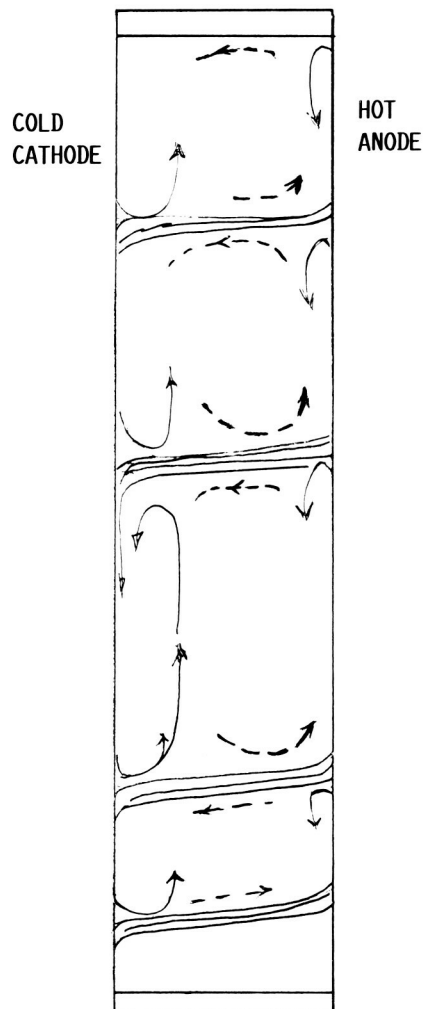
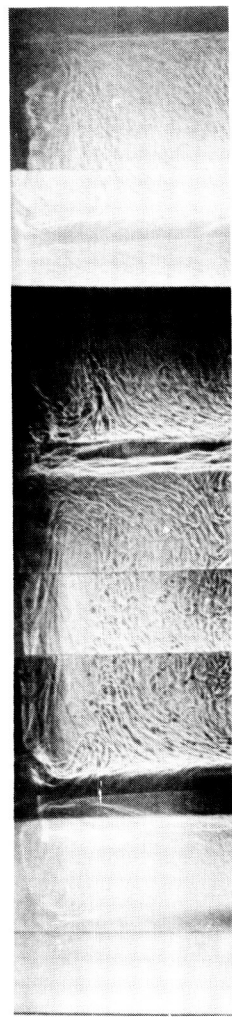


FIGURE 4. - FLOW STRUCTURE FOR OPPOSING CASE WITH $Ar = 7$,
 $Gr_T = 4.84 \times 10^8$, $Gr_S = 3.89 \times 10^8$.

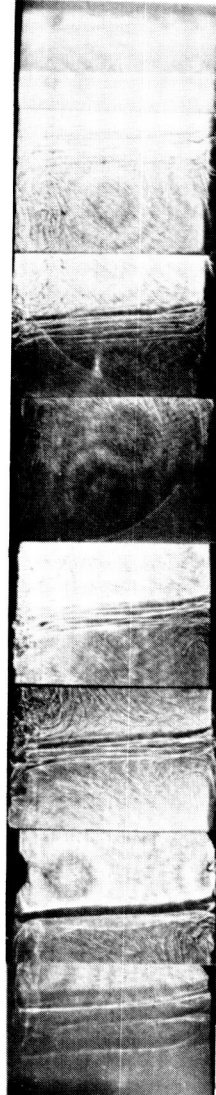
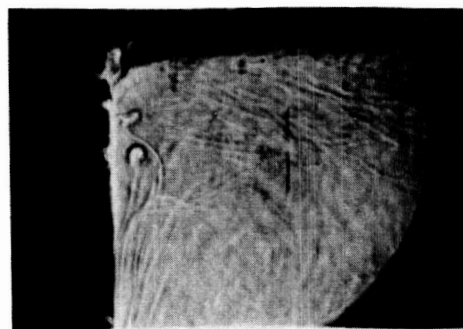


FIGURE 5. - FLOW STRUCTURE FOR OPPOSING CASE WITH
 $Ar = 7$, $Gr_T = 7.75 \times 10^7$, $Gr_S = 3.89 \times 10^8$.

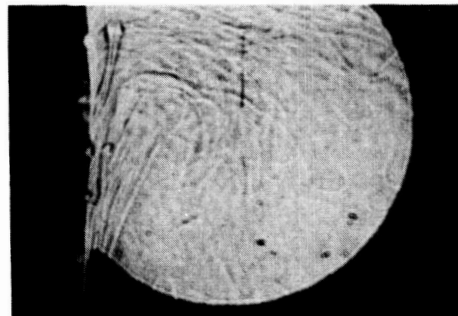


ORIGINAL PAGE IS
OF POOR QUALITY

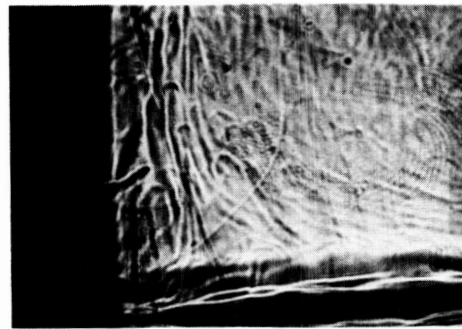
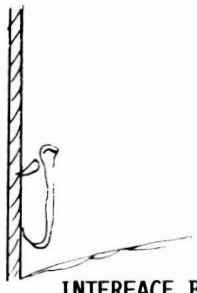
INTERFACE A



(a) $Gr_T = 5.01 \times 10^7$.



(b) $Gr_T = 1.01 \times 10^8$.

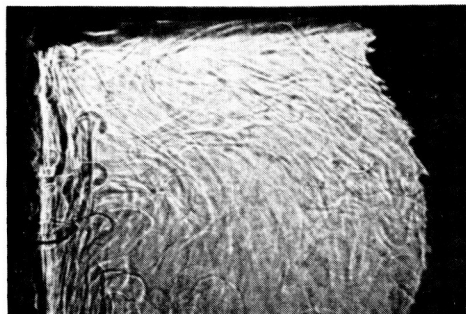


INTERFACE B

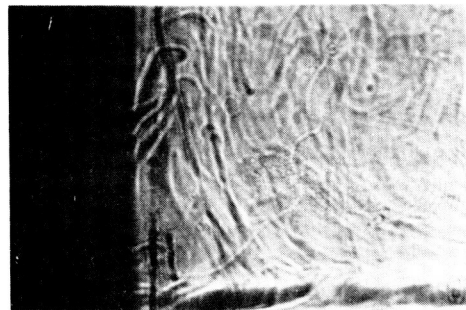
(c) $Gr_T = 2.02 \times 10^8$.

FIGURE 6. - NEAR-FIELD FLOW STRUCTURE AROUND THE COLD ANODE
FOR COOPERATING CASE WITH $Ar = 3$, $Gr_S = 1.52 \times 10^7$ (THE
POSITION OF INTERFACE A IS HIGHER THAN THE POSITION OF
INTERFACE B).

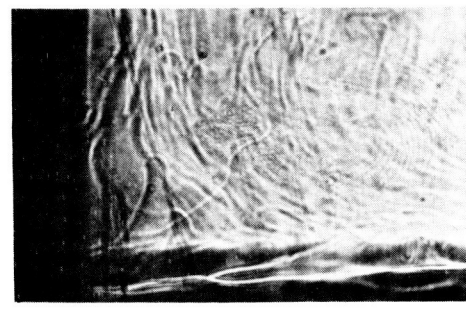
INTERFACE A



$$(a) Gr_T = 1.34 \times 10^8.$$



$$(b) Gr_T = 2.68 \times 10^8.$$

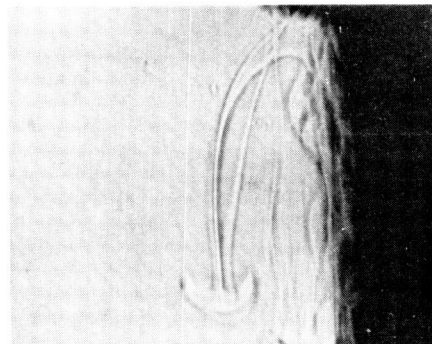


INTERFACE B

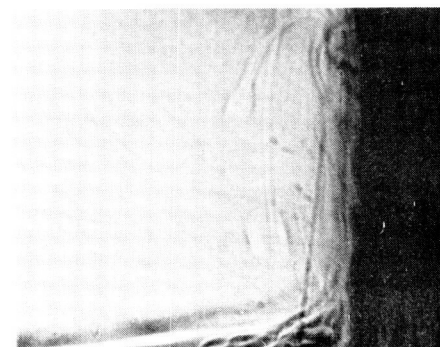
$$(c) Gr_T = 4.03 \times 10^8.$$

FIGURE 7. - NEAR-FIELD FLOW STRUCTURE AROUND THE COLD ANODE FOR COOPERATING CASE WITH $Ar = 7$, $Gr_S = 1.28 \times 10^9$ (THE POSITION OF INTERFACE A IS HIGHER THAN THE POSITION OF INTERFACE B).

INTERFACE A

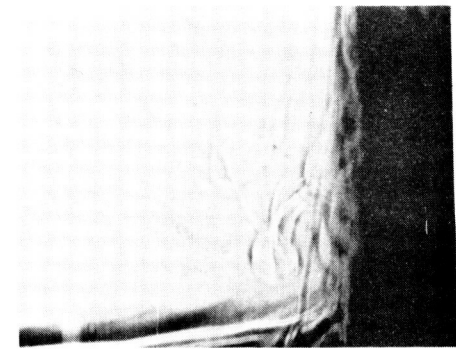


$$(a) Gr_T = 5.01 \times 10^8.$$



INTERFACE B

$$(b) Gr_T = 2.68 \times 10^8.$$



INTERFACE B

$$(c) Gr_T = 1.34 \times 10^8.$$

FIGURE 8. - NEAR-FIELD FLOW STRUCTURE AROUND THE HOT ANODE FOR OPPOSING CASE WITH $Ar = 7$, $Gr_S = 1.28 \times 10^9$ (THE POSITION OF INTERFACE A IS HIGHER THAN THE POSITION OF INTERFACE B).

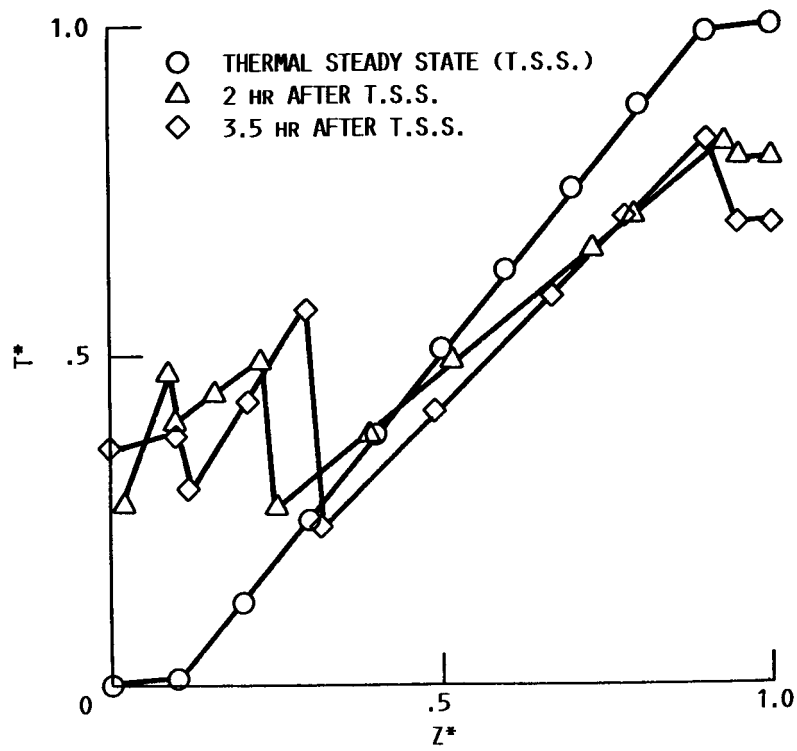


FIGURE 9. - CHANGES OF TEMPERATURE PROFILE AT MID-
SECTION FOR COOPERATING CASE WITH $Ar = 7$,
 $Gr_T = 1.34 \times 10^8$, $Gr_S = 1.28 \times 10^9$. $x^* = 0.5$,
 $y^* = 0.5$.

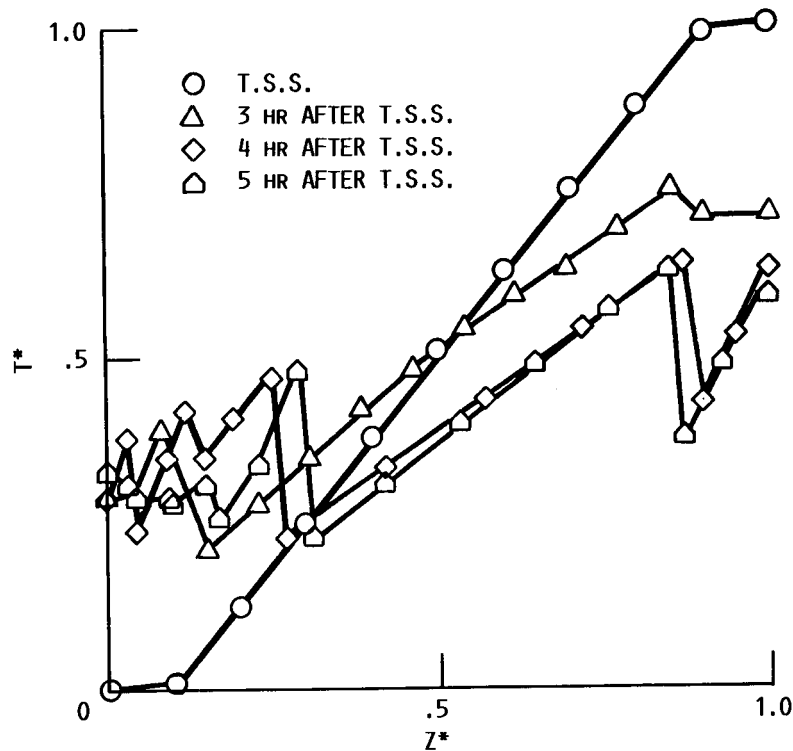


FIGURE 10. - CHANGES OF TEMPERATURE PROFILE AT MID-
SECTION FOR OPPOSING CASE WITH $Ar = 3$, $Gr_T =$
 5.01×10^7 , $Gr_S = 1.52 \times 10^7$. $x^* = 0.5$, $y^* = 0.5$.



National Aeronautics and
Space Administration

Report Documentation Page

1. Report No. NASA TM-100803	2. Government Accession No.	3. Recipient's Catalog No.	
4. Title and Subtitle Thermosolutal Convection in High-Aspect-Ratio Enclosures		5. Report Date	
6. Performing Organization Code		7. Author(s) L.W. Wang and C.T. Chen	
8. Performing Organization Report No. E-3881		9. Performing Organization Name and Address National Aeronautics and Space Administration Lewis Research Center Cleveland, Ohio 44135-3191	
10. Work Unit No. 674-24-05		11. Contract or Grant No.	
12. Sponsoring Agency Name and Address National Aeronautics and Space Administration Washington, D.C. 20546-0001		13. Type of Report and Period Covered Technical Memorandum	
14. Sponsoring Agency Code		15. Supplementary Notes Prepared for the 25th National Heat Transfer Conference sponsored by the American Society of Mechanical Engineers, Houston, Texas, July 24-27, 1988. L.W. Wang, National Research Council - NASA Research Associate, on leave from the Institute of Aeronautics and Astronautics, National Cheng Kung University, Taiwan, Republic of China; C.T. Chen, Institute of Aeronautics and Astronautics, National Cheng Kung University.	
16. Abstract Convection in high-aspect-ratio rectangular enclosures with combined horizontal temperature and concentration gradients is studied experimentally. An electrochemical system is employed to impose the concentration gradients. The solutal buoyancy force either opposes or augments the thermal buoyancy force. Due to a large difference between the thermal and solutal diffusion rates the flow possesses double-diffusive characteristics. Various complex flow patterns are observed with different experimental conditions.			
17. Key Words (Suggested by Author(s)) Heat transfer Thermal convection		18. Distribution Statement Unclassified - Unlimited Subject Category 34	
19. Security Classif. (of this report) Unclassified	20. Security Classif. (of this page) Unclassified	21. No of pages 14	22. Price* A02